Effects of Mutations and Complex Formation on the Reduction Potentials of Cytochrome *c* and Cytochrome *c* Peroxidase

Huan-Xiang Zhou

Contribution from the Laboratory of Chemical Physics, National Institute of Diabetes and Digestive and Kidney Diseases, National Institutes of Health, Bethesda, Maryland 20892

Received December 13, 1993. Revised Manuscript Received May 27, 1994[⊗]

Abstract: A continuum model is used to calculate the effects of point mutations and complex formation on the reduction potentials of yeast iso-1-cytochrome *c* (cc) and yeast cytochrome *c* peroxidase (CCP). In this model a protein is represented by a low dielectric region embedded in the high dielectric solvent. Qualitative analysis shows that the model can account for a wide range of factors that determine the reduction potential. These include the charge and polarity of a surface residue, the polarity of an interior residue, and the size of a residue which controls the exposure of the heme to the solvent. The continuum model allows for a reasonably good reproduction of a demanding set of data on cc, consisting of the measured differences in reduction potential between the wild type and seven mutants (Arg38 → Lys, His, Asn, and Ala, Tyr48 → Phe, Asn52 → Ile, and Phe82 → Ser). In the case of CCP, continuum-model calculations on the effects of mutating Asp235 lead to the following conclusions: (1) The imidazolate character of wild-type His175, shown by resonance Raman spectroscopy and NMR, is critical in lowering the reduction potential of the wild type 70 mV from that of the Glu235 mutant, which has the same charge as the wild type. (2) A sixth ligand, such as a water molecule, is necessary for maintaining the reduction potential of the Ala235 mutant at a level that is only 35 mV above the reduction potential of the Glu235 mutant, which has an extra buried carboxylate. (3) That the Asn235 and Ala235 mutants have almost equal reduction potentials is due to the fact that the amide dipole of the Asn235 residue is oriented such that it does not stabilize or destabilize the charge on the heme. In contrast to previous expectations, complex formation is found to have only a small effect on the reduction potential of cc and no effect at all on that of CCP. The protein matrices are found to play an important role of reducing the outer reorganization energy from what would have been if the redox centers were embedded directly in the solvent and thus speeding up the electron transfer. By relating electron transfer to redox reactions, a method for obtaining the inner reorganization energy is proposed.

I. Introduction

The reduction potential of an electron-transfer protein provides the driving force for this biochemical reaction. After the introduction of site-directed mutagenesis, yeast iso-1-cytochrome *c* (cc) has become a paradigm in which factors that affect the reduction potential are explored.[1] Changes in reduction potential due to point mutations at various sites of this protein were measured, and several different factors have been proposed to explain these results. These include heme exposure to solvent,[2−5] charges on ionized groups,[3,6,7] and dipoles of interior polar groups.[8] By now it is clear that different factors may operate under different circumstances and no single factor is dominant. It becomes very desirable to have a unified model which allows one to both qualitatively and quantitatively predict the effects of the various factors on the reduction potential.

The reduction potential E for the redox reaction

$$O + e^- \rightleftarrows R \tag{1}$$

is governed by the Nernst equation

$$E = E^{\circ\prime} + \frac{k_B T}{ef} \ln \frac{[R]}{[O]} \tag{2}$$

where $E^{\circ\prime}$ is the standard potential, [O] and [R] are the concentrations of the oxidized and reduced species, respectively, $k_B T$ is the product of Boltzmann's constant and the temperature, e is the unit charge, and f is a factor for the conversion between two units of energy, eV and kcal/mol (1 eV = 23.1 kcal/mol). The standard potential $E^{\circ\prime}$ is related to the difference in standard chemical potential between the oxidized and reduced states[9]

$$efE^{\circ\prime} = \Delta\mu^\circ \equiv \mu^\circ_O - \mu^\circ_R \tag{3}$$

where again the factory f is inserted to take care of unit conversion between $eE^{\circ\prime}$, which is in eV, and $\Delta\mu^\circ$, which is in kcal/mol. One can partition $\Delta\mu^\circ$, the change in standard chemical potential upon oxidation, into three major terms.[10] The first, $\Delta\mu^\circ_{cen}$, is due to the change in bonding interactions at the redox center. The second, $\Delta\mu^\circ_{el}$, arises from the electrostatic interactions of the redox-center charge with polar and ionized groups of the protein and the solvent. A third term, $\Delta\mu^\circ_{conf}$, resulting from conformational changes upon oxidation, is often expected to be negligible for simple electron-transfer proteins. This paper deals with the effects of changing the protein environment on the reduction potential. The environmental change is due either to a point mutation or to complex formation. As the same redox center is involved, the effect on the reduction

⊗ Abstract published in *Advance ACS Abstracts*, October 1, 1994.

(1) Mauk, A. G. *Struct. Bonding* **1991**, *75*, 131−157.
(2) Kassner, R. J. *Proc. Natl. Acad. Sci. U.S.A.* **1972**, *69*, 2263−2267.
(3) Churg, A. K.; Warshel, A. *Biochemistry* **1986**, *25*, 1675−1681.
(4) Louie, G. V.; Pielak, G. J.; Smith, M.; Brayer, G. D. *Biochemistry* **1988**, *27*, 7870−7876.
(5) Rafferty, S. P.; Pearce, L. L.; Barker, P. D.; Guillemette, J. G.; Kay, C. M.; Smith, M.; Mauk, A. G. *Biochemistry* **1990**, *29*, 9365−9369.
(6) Schejter, A.; Eaton, W. A. *Biochemistry* **1984**, *23*, 1081−1084.
(7) Cutler, R. L.; Davies, A. M.; Creighton, S.; Warshel, A.; Moore, G. R.; Smith, M.; Mauk, A. G. *Biochemistry* **1989**, *28*, 3188−3197.
(8) Langen, R.; Brayer, G. D.; Berghuis, A. M.; McLendon, G.; Sherman, F.; Warshel, A. *J. Mol. Biol.* **1992**, *224*, 589−600.
(9) Bard, A. J.; Faulkner, L. R. *Electrochemical Methods*; John Wiley & Sons: New York, 1980.
(10) Moore, G. R.; Pettigrew, G. W.; Rogers, N. K. *Proc. Natl. Acad. Sci. U.S.A.* **1986**, *83*, 4998−4999.

potential mainly comes from the change, $\Delta\Delta\mu^\circ_{el}$, in the electrostatic interactions of the redox center with the protein environment (including the solvent). Consequently the resulting change in reduction potential, $\Delta E^{\circ\prime}$, is given by

$$ef\Delta E^{\circ\prime} = \Delta\Delta\mu^\circ_{el} \quad (4)$$

(The above formulation neglects the effects of activity coefficients. These effects should vary little when the protein environment is changed upon a point mutation or complex formation and thus should contribute insignificantly to $\Delta E^{\circ\prime}$.) The redox center of every protein considered will be a heme.

The paper has three purposes. First, we would like to see whether a dielectric continuum model for proteins is capable of quantitatively reproducing the wide-ranging effects of point mutations on the reduction potential of cc. In the dielectric continuum model, a protein is represented by a low dielectric region embedded in the high dielectric solvent. In a pioneering work, Rogers, Moore, and Sternberg[11] used this model to study the effect of ionizing a buried heme propionic acid on the reduction potential of cytochrome c_{551}. More recently, the continuum model has been used to study the differences in the reduction potentials of four redox sites in a photosynthetic reaction center.[12,13] There the redox centers are buried in completely different protein matrices and the spread of the reduction potentials is rather wide (~440 mV). The changes in reduction potential due to point mutations are rather small (usually less than 50 mV, corresponding to a change in free energy of about 1 kcal/mol), and the effects are much subtler.

After establishing the capability of the dielectric continuum model in reproducing the effects of point mutations on the reduction potential of cc, we use this model to understand the recent results of Goodin and McRee[14] concerning the effects of mutating an interior residue, Asp235, into another charged, polar, or nonpolar residue on the reuction potential of yeast cytochrome *c* peroxidase (CCP). These results demonstrate effects of point mutations that apparently are very different from what were found in cc. In cc, a mutation of Arg38 → Lys (both positively charged) resulted in a small decrease of 23 mV in the reduction potential $E^{\circ\prime}$.[7] On the other hand, a mutation Asp235 → Glu (both negatively charged) in CCP resulted in a large increase of 70 mV in $E^{\circ\prime}$. In addition, the mutation Asn52 → Ile, from a polar to a nonpolar residue at an interior position in cc gave rise to a large decrease of 55 mV in $E^{\circ\prime}$,[8,15] whereas the reduction potentials were virtually identical ($\Delta E^{\circ\prime}$ = 1 mV) for two CCP mutants in which an Asn residue and a nonpolar Ala residue occupy the interior position 235. Understanding these differences helps us gain knowledge on the diversity of protein structure and function.

Ultimately a redox protein utilizes its reduction potential to drive electron transfer. Prior to electron transfer, the donor protein has to form a complex with the acceptor protein. The third purpose of this paper is to find out how complex formation would influence the reduction potentials of the proteins. Rees[16] and Moore, Pettigrew, and Rogers[10] have suggested that, to facilitate electron transfer, the changes in protein environment upon complex formation (e.g., neutralization of oppositely charged residues) would change the $\Delta\mu^\circ_{el}$ values of both the donor and the acceptor so as to equalize their reduction potentials. With the X-ray structure of the complex between cc and CCP now available,[17] we can assess this suggestion. What we found was in direct contradiction with this suggestion. Complex formation has rather minor effects on the reduction potentials: it lowered $E^{\circ\prime}$ of cc by ~40 mV and did not affect $E^{\circ\prime}$ of CCP at all. This finding is supported by the experimental results of Vanderkooi and Erecinska[18] and Burrows *et al.*[15] The former group found that complex formation with either CCP or cytochrome b_5 did not cause any measurable change in the reduction potential of cc. The latter group studied the complex formation between cc and cytochrome b_5 and observed that upon complexation the reduction potential of either protein changed by less than 20 mV. Further support comes from the experimental observation that reduced (Fe^{2+}) and oxidized (Fe^{3+}) cc's have very similar affinities to CCP.[19,20]

In the classical electron-transfer theory of Marcus,[21-23] the reorganization that has to occur before the transfer of an electron was separated into two parts, an inner part involving bond rearrangement of the redox centers and an outer part involving polarization reorientation of the surrounding environment. The total reorganization energy is the sum of the two contributions:

$$\lambda = \lambda_i + \lambda_o \quad (5)$$

This separation implies that λ_i should be related to the $\Delta\mu^\circ_{cen}$ term of $\Delta\mu^\circ$, the change in standard chemical potential for a redox reaction, and λ_o should be related to the $\Delta\mu^\circ_{el}$ term of $\Delta\mu^\circ$. The Marcus theory for λ_o is usually implemented in a dielectric continuum model, and this implementation has been very successful for dealing with electron transfer in small molecules, where the outer reorganization occurs primarily in the solvent. However, it is still not clear what is the proper way to find λ_o in a continuum model for biological electron transfer, which involves also the reorganization of intervening protein matrices.[23] In addition, the inner reorganization of biological electron transfer is much more complex. In the final part of the paper we also present our attempt to find ways for obtaining the inner and outer reorganization energies and analyze experimental results for the electron transfer between cc and CCP[24] and the self-exchange in cc.[26]

(11) Rogers, N. K.; Moore, G. R.; Sternberg, M. J. E. *J. Mol. Biol.* **1985**, *182*, 613–616.
(12) Zheng, C.; Davis, M. E.; McCammon, J. A. *Chem. Phys. Lett.* **1990**, *173*, 246–252.
(13) Gunner, M. R.; Honig, B. *Proc. Natl. Acad. Sci. U.S.A.* **1991**, *88*, 9151–9155.
(14) Goodin, D. B.; McRee, D. E. *Biochemistry* **1993**, *32*, 3313–3324.
(15) Burrows, A. L.; Guo, L. H.; Hill, H. A. O.; McLendon, G.; Sherman, F. *Eur. J. Biochem.* **1991**, *202*, 543–549.
(16) Rees, D. C. *Proc. Natl. Acad. Sci. U.S.A.* **1985**, *82*, 3082–3085.
(17) Pelletier, H.; Kraut, J. *Science* **1992**, *258*, 1748–1755.
(18) Vanderkooi, J.; Erecinska, M. *Arch. Biochem. Biophys.* **1974**, *162*, 385–391.
(19) Leonard, J. J.; Yonetani, T. *Biochemistry* **1974**, *13*, 1465–1468.
(20) McLendon, G.; Zhang, Q.; Wallin, S. A.; Miller, R. M.; Billstone, V.; Spears, K. G.; Hoffman, B. M. *J. Am. Chem. Soc.* **1993**, *115*, 3665–3669.
(21) Marcus, R. A. *J. Chem. Phys.* **1965**, *43*, 679–701.
(22) Brown, G. M.; Sutin, N. *J. Am. Chem. Soc.* **1979**, *101*, 883–892.
(23) Marcus, R. A.; Sutin, N. *Biochim. Biophys. Acta* **1985**, *811*, 265–322.
(24) Cheung, E.; Taylor, K.; Kornblatt, J. A.; English, A. M.; McLendon, G.; Miller, J. R. *Proc. Natl. Acad. Sci. U.S.A.* **1986**, *83*, 1300–1333. These authors measured the rates k_{et} of electron transfer from ferro-CCP to ferri-cc and from the anion radical of H_2 porphyrin cc to ferri-CCP and found k_{et} to be about 1 and 150 s^{-1}, respectively. In the Marcus theory, k_{et} is related to the reorganization energy through $-k_BT \ln k_{et} = (-ef\Delta E^{\circ\prime} + \lambda)^2/4\lambda$ + constant, where $\Delta E^{\circ\prime}$ is the difference in reduction potential between the acceptor and the donor. The reduction potentials are those for the proteins in complex but should be close to those for the proteins in isolation, since the present work shows that the effects of complex formation on reduction potential are rather minor. The reduction potentials of cc and CCP in isolation are about 270 and −190 mV, respectively, while the potential for the reduction of H_2 porphyrin cc to the anion radical has been measured to be −1100 mV.[25] Thus $\Delta E^{\circ\prime}$ is 460 mV for the electron transfer from CCP to cc and 910 mV from the electron transfer from H_2 porphyrin cc to CCP. Using these values of $\Delta E^{\circ\prime}$ and the values of k_{et} given earlier, one finds λ = 37 kcal/mol.

The outline for the rest of the paper is as follows. In section II we describe the dielectric continuum model and the calculation of the reduction potential. We then present results on the changes in reduction potential due to mutations at four positions of cc in section III. The Arg38 → Lys, His, Asn, and Ala mutations illustrate the effect of the charge and polarity of a surface residue, the Tyr48 → Phe and Asn52 → Ile mutations illustrate the effect of the polarity of an interior residue, and the Phe82 → Ser mutation illustrates the effect of the size of a residue which controls the exposure of the heme to the solvent. In section IV we calculate the effects of mutating Asp235 in CCP. The effects of complex formation on the reduction potentials of cc and CCP are described in section V. Also presented there are our method for obtaining the reorganization energy and the results for two electron-transfer reactions. Finally we make some concluding remarks in section VI.

II. The Dielectric Continuum Model

As mentioned in the Introduction, in the dielectric continuum model, a protein is represented by a low dielectric region embedded in the high dielectric solvent. This model originates from the work of Tanford and Kirkwood,[27] who used a sphere to represent the protein. This allowed them to find an analytical solution for the electrostatic potential. In recent years Warwicker and Watson[28] extended the spherical model by using the X-ray structure of the protein for the dielectric boundary between the protein and the solvent. The equations for the electrostatic potential cannot be solved analytically anymore, and one has to resort to a numerical method.

A. Spherical Model. To illustrate the behaviors of the dielectric continuum model that incorporates the X-ray structure of a protein in dealing with factors that determine the reduction potential, we first examine a spherical model. As a spherical model is analytically solvable, such an examination allows us to gain intuition on these factors. This is an advantage of the continuum model over microscopic models such as the protein dipole Langevin dipole (PDLD) model of Warshel and coworkers.[7,8] In the particular spherical model that we use, the redox center is represented by a point located at the center of the sphere. While different authors have used the spherical model to emphasize a different factor,[2,3,6] here we use this model to discuss several factors that have been identified as important in determining the reduction potential of cc (see the Introduction). These factors are the charge of an ionizable group, the dipole of an interior polar residue, and the size of a residue which controls the exposure of the redox center to the solvent.

Let the charges of the protein be $\{q_l\}$, and let their distances to the redox center be $\{r_l\}$. If the electrostatic potentials at the lth charge site are V_l^O and V_l^R in the oxidized and reduced states, respectively, and the electrostatic potential at the redox center of the oxidized species is V_{cen}, then the electrostatic contribution to the change in standard chemical potential upon oxidation is

$$\Delta\mu^\circ_{el} = eV_{cen}/2 + \sum_l q_l(V_l^O - V_l^R)/2 \tag{6}$$

The difference $\Delta V_l \equiv V_l^O - V_l^R$ is generated by the charge e at the redox center of the oxidized species (for this statement to be valid, it is assumed that the structure of the protein is unchanged upon oxidation, i.e., the only difference between the oxidized and reduced species is the extra charge e at the redox center). ΔV_l has two components. The first is the direct action of e,

$$\Delta V_l^d = e/\epsilon_i r_l \tag{7}$$

where ϵ_i is the dielectric constant of the protein interior. The second component is the reaction field due to the dielectric boundary between the protein and the solvent. For the spherical model, this is

$$\Delta V_l^r = -(1/\epsilon_i - 1/\epsilon)e/a \tag{8}$$

where a is the radius of the protein and ϵ is the dielectric constant of the solvent. Notice that ΔV_l^r is uniform over the interior of the sphere.

The electrostatic potential V_{cen} at the redox center of the oxidized species is generated by both the protein charges $\{q_l\}$ (contribution $V_{cen,l}$) and the charge e at the redox center (contribution $V_{cen,cen}$). By symmetry one has

$$eV_{cen,l} = q_l\Delta V_l \tag{9}$$

$V_{cen,cen}$ again has a direct-action component and a reaction-field component. The first component, the self-energy of e, is infinite, but this poses no problem because we will be interested in the difference in $\Delta\mu^\circ_{el}$ due to a mutation or complex formation and it will be canceled upon taking the difference. The reaction-field component is again given by eq 8. After summing up the various terms (neglecting the self-energy of e), one has

$$\Delta\mu^\circ_{el} = -(1/\epsilon_i - 1/\epsilon)e^2/2a + \sum_l eq_l/\epsilon_i r_l - (1/\epsilon_i - 1/\epsilon)eQ/a \tag{10}$$

where $Q = \sum_l q_l$ is the total charge in the reduced state.

We are now in a position to discuss the various factors that determine the reduction potential. For this purpose we will use dielectric constants of $\epsilon_i = 4$ for the protein and $\epsilon = 78.5$ for the solvent. First let us consider the effect on the reduction potential due to the charge of an ionizable group. If the charge at the first site changes from zero to q_l upon a point mutation or ionization, the resulting change in $\Delta\mu^\circ_{el}$ is

$$\Delta\Delta\mu^\circ_{el} = eq_1/\epsilon_i r_1 - (1/\epsilon_i - 1/\epsilon)eq_1/a \tag{11}$$

The first term is due to the direct action of q_1, and the second term is due to the reaction field from the dielectric boundary. Note that, as $\epsilon \gg \epsilon_i$, the second term has a sign that is opposite to that of the first term and a magnitude that is smaller than that of the first term by a factor of roughly r_1/a. If q_1 is close to the dielectric boundary (i.e., $r_1 \approx a$), then the reaction field largely offsets the effect of the direct action and the overall contribution of q_1 to the reduction potential is small. This is equivalent to having a high effective dielectric constant for the interaction of the redox center with q_1.

For concreteness, let us look at the case of ionizing the buried heme propionic acid in cytochrome c_{551}. The appropriate parameters for this case are[11] $q_1 = -e$, $r_1 = 8.25$ Å, and $a = 13.25$ Å. If only the direct action of the propionate charge gained upon ionization is considered, one obtains $\Delta\Delta\mu^\circ_{el} = eq_1/\epsilon_i r_1 = -10.1$ kcal/mol. This would predict a decrease of 436

(25) McLendon, G.; Miller, M. R. *J. Am. Chem. Soc.* **1985**, *107*, 7811–7816.

(26) (a) Gupta, R. *Biochim. Biophys. Acta* **1973**, *292*, 291–295. By Arrhenius-plot analysis of NMR data, the activation enthalpy, which is $\lambda/4$ for a self-exchange reaction,[23] was found in this work to be 7 ± 1 kcal/mol for the cc self-exchange. (b) Nocera, D. G.; Winkler, J. R.; Yocom, K. M.; Bordignon, E.; Gray, H. B. *J. Am. Chem. Soc.* **1984**, *106*, 5145–5150. Using relations between a cross reaction and the component self-exchange reactions, these authors again found $\lambda/4$ to be 7 kcal/mol.

(27) Tanford, C.; Kirkwood, J. G. *J. Am. Chem. Soc.* **1979**, *79*, 5333–5339.

(28) Warwicker, J.; Watson, H. C. *J. Mol. Biol.* **1982**, *157*, 671–679.

mV in reduction potential. When the effect of the reaction field is included, the contribution of the propionate is estimated to be a decrease of only 178 mV (corresponding to an effective dielectric constant of 10). In comparison, the detailed calculations of Rogers, Moore, and Sternberg[11] found a decrease of 90 mV and the experimental result is 65 mV (corresponding to an effective dielectric constant of 27). The spherical model thus demonstrates the ability of the dielectric continuum model to generate a high effective dielectric constant.

Next we consider the effect on the reduction potential due to the dipole on the side chain of a polar residue. Suppose a polar residue is mutated into a nonpolar one. If the polar side chain has partial charges $\{q_{l'}\}$ ($\sum_{l'} q_{l'} = 0$) and the nonpolar side chain has no partial charges, then the change in $\Delta\mu^\circ_{el}$ upon mutation is

$$\Delta\Delta\mu^\circ_{el} = -\sum_{l'} eq_{l'}/\epsilon_i r_{l'} \tag{12a}$$

$$\approx -e\mathbf{p}\cdot\mathbf{r}/\epsilon_i r^3 \tag{12b}$$

where $\mathbf{p}$ is the dipole moment of the polar side chain and $\mathbf{r}$ is the vector from somewhere inside the side chain to the redox center.

As an example, let us look at the mutation of Tyr48 → Phe in cc. The extra hydroxyl group on the Tyr residue, which forms a hydrogen bond to a heme propionate, results in a dipole moment of ~0.44 eÅ. The dipole moment has a distance of ~9 Å away from the heme iron and an angle of only ~30° away from directly pointing at the heme iron (how these parameters are obtained will be discussed later). Using these parameters, one obtains $\Delta\Delta\mu^\circ_{el} = -0.39$ kcal/mol. This amounts to a decrease of 17 mV in reduction potential, which is close to the experimental result of 22 mV of Davis *et al.*[29] These authors have proposed that this decrease in reduction potential was caused by increased electron density on the heme propionate due to the loss of the hydrogen bond with Tyr48 upon mutation. The above analysis suggests that no such elaborate scheme is required to explain the experimental result and the decrease in reduction potential can come about simply due to the loss of the hydroxyl dipole of Tyr48.

Finally we use the spherical model to discuss the effect on the reduction potential due to the size of a residue which controls the exposure of the redox center to the solvent. A change in the size of such a residue necessarily brings us to a nonspherical geometry; thus, the spherical model is not quite appropriate for discussing this factor. Nonetheless we will look at the case in which the solvent exposure of the redox center is increased due to a uniform shrinkage of the spherical surface and deduce what happens after a localized increase in the solvent exposure upon a point mutation. The change in $\Delta\mu^\circ_{el}$ due to a decrease in the radius of the protein from a to $a - \delta$ is

$$\Delta\Delta\mu^\circ_{el} = -(1/\epsilon_i - 1/\epsilon)e^2/2a(a/\delta - 1) - (1/\epsilon_i - 1/\epsilon)eQ/a(a/\delta - 1) \tag{13}$$

The first term is due to increased exposure of the redox center to the solvent, and the second term is due to increased screening of the redox center–protein interactions by the solvent. While the first contribution to $\Delta\Delta\mu^\circ_{el}$ has attracted a lot of attention,[2-5] the second contribution does not appear to have been specifically discussed. Depending on the sign and magnitude of the total charge Q, the second contribution may either enhance or depress

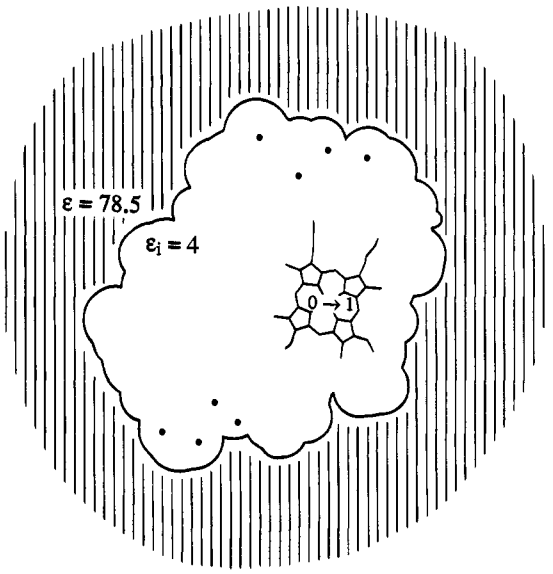

Figure 1. Continuum model for calculating the reduction potential of a heme protein. The transition "0 → 1" at the heme iron denotes the changes of heme partial charges upon oxidation. Closed circles represent charges on the atoms of the protein matrix.

and may dominate the effect of the increased solvent exposure of the redox center. The spherical model thus helps bring out this important contribution to the change in reduction potential. In the case that a localized increase in the solvent exposure of the redox center occurs due to a point mutation, the charges in the neighborhood of the mutation, rather than the total charge Q, enter into the discussion.

B. Detailed Model. Having discussed the qualitative behaviors through analysis of the spherical model, we now describe the detailed continuum model in which the X-ray structure, rather than a sphere, is used to determine the dielectric boundary between the protein and the solvent (see Figure 1). A further generalization in the detailed model is that the charge gained upon oxidation may be spread over the heme rather than localized at a single site. Thus we have two charge distributions, $\{q_l^R\}$ and $\{q_l^O\}$, one for the reduced state and the other for the oxidized state (of course, $Q^O - Q^R = \sum_l q_l^O - \sum_l q_l^R = e$). The electrostatic potential inside the protein, in either the reduced or the oxidized state, satisfies Poisson's equation

$$\nabla^2 V(\mathbf{r}) = -4\pi \sum_l q_l \delta(\mathbf{r} - \mathbf{r}_l)/\epsilon_i \tag{14}$$

The last generalization in the detailed model is that salt ions may be present in the solvent. They are taken into consideration by the Poisson–Boltzmann equation

$$\nabla^2 V(\mathbf{r}) - \kappa^2 V(\mathbf{r}) = 0 \tag{15}$$

for the electrostatic potential in the solvent. Here the Debye screening constant κ is given by $\kappa^2 = 8\pi I e^2/\epsilon k_B T$, in which I is the ionic strength.

The electrostatic contribution to the change in standard chemical potential upon oxidation is a generalization of eq 6:

$$\Delta\mu^\circ_{el} = \sum_l (q_l^O V_l^O - q_l^R V_l^R)/2 \tag{16}$$

where V_l^O and V_l^R are the electrostatic potentials at the lth site in the oxidized and reduced states, respectively. To separate the contribution due to the dielectric boundary from that due to the direct charge–charge interactions, we again partition the electrostatic potential at each charge site into a direct-action

(29) Davies, A. M.; Guillemette, J. G.; Smith, M.; Greenwood, C.; Thurgood, A. G. P.; Mauk, A. G.; Moore, G. R. *Biochemistry* **1993**, *32*, 5431–5435.

component and a reaction-field component. Here

$$V_l^{\mathrm{d}} = -\sum_{l'} q_{l'}/\epsilon_{\mathrm{i}}|\mathbf{r}_l - \mathbf{r}_{l'}| \qquad (17)$$

and V_l^{r} has to be found by solving the Poisson and Poisson–Boltzmann equations (eqs 14 and 15). In the summation of eq 17, the infinite self-potential at each charge site should be excluded. For a non-heme site, $q_l^{\mathrm{O}} = q_l^{\mathrm{R}}$ and thus the self-potentials from the oxidized and reduced states will cancel out each other in calculating $\Delta\mu^\circ_{\mathrm{el}}$; for a heme site, $q_l^{\mathrm{O}} \neq q_l^{\mathrm{R}}$ and the self potentials do not cancel out but their net effect will cancel out when the change in $\Delta\mu^\circ_{\mathrm{el}}$ upon a mutation or complex formation is calculated. By summing the direct-action components and the reaction-field components respectively over all the charge sites, one obtains the direct-action contribution $\Delta\mu^\circ_{\mathrm{d}}$ and the reaction-field contribution $\Delta\mu^\circ_{\mathrm{r}}$ to $\Delta\mu^\circ_{\mathrm{el}}$.

The numerical method for solving the Poisson and Poisson–Boltzmann equations deserves some comments. Most workers[11-13,28] have used the finite-difference method, in which the infinite three-dimensional space is represented by a finite cubic lattice. We have developed an alternative method based on the boundary-element technique, in which the Poisson and Poisson–Boltzmann equations are transformed into integral equations on the protein surface.[30-32] The boundary-element method allows one to have an accurate description of the protein surface and to have charges located exactly. These two features are important in reducing numerical errors, which are of particular concern in studying the effects of point mutations on reduction potential as the involved changes in energy are rather small. In addition, the boundary-element method allows us to easily treat the large system presented by the complex formed between cc and CCP. Because of these considerations, this method was chosen for the present work.

In the calculations, the charges used for the amino acids were from the OPLS parameters,[33] in which partial charges are assigned to heavy atoms and polar hydrogens. The charges for the reduced (Fe^{2+}) heme were taken from the work of Northrup *et al.*[34] The charges for the oxidized (Fe^{3+}) heme were obtained by adding to those of the reduced heme the changes of partial charges upon oxidation found by Churg *et al.*[35] These oxidation-induced charge changes are from quantum mechanical calculations and include the effect of the protein matrix of cc. To check the sensitivity of the calculated results to these charge changes, calculations were also made using other distributions for the charge gained upon oxidation. The total charge on reduced cc is $Q^{\mathrm{R}} = 6e$; for CCP, $Q^{\mathrm{R}} = -13e$.

The positions of the heavy atoms were taken from the X-ray structure of each protein, while the positions of polar hydrogens were generated from the positions of neighboring heavy atoms using standard geometries. The following radii were used to generate the surface of a protein: C, 2.0 Å; N, 1.7 Å; O, 1.5 Å; S, 1.8 Å; Fe, 1.7 Å; H, 1.0 Å. The protein dielectric constant ϵ_{i} was 4, and the solvent dielectric constant ϵ was taken as the value for water at the appropriate temperature. It is 78.5 at T = 298 K and 82.3 at T = 288 K.

The quantity of interest in the present work is the change in reduction potential due to a point mutation or complex formation. This is given by $\Delta\Delta\mu^\circ_{\mathrm{el}}$, the *difference* in the *change* of the electrostatic interactions of the redox center with the protein environment; the change results from oxidation, and the difference arises from a point mutation or complex formation. As the final result involves two netted processes of calculating energy differences, one has to make sure that errors in the involved quantities are properly canceled out. Numerical errors were just mentioned, but additional errors may come from the particular charges and atomic positions used. To minimize the latter category of errors in the first process of calculating energy difference, the one involving oxidation, we used the same structure for both the reduced and the oxidized states of a protein (as for charges, the amino acid part of the protein had no changes upon oxidation, while the heme had changes as described above). In the second process of calculating energy difference, the one involving a point mutation or complex formation, only X-ray structures that are of high resolution were used. For each mutant that has no high-resolution X-ray structure, we built its structure by planting the mutation in the wild-type structure so that the mutant and the wild type had the same structure except for the residue that was mutated. This would single out the effect of the mutation. With these considerations in mind, we now present the calculated results on the effects of point mutations and complex formation in cc and CCP.

III. Point Mutations in Yeast Iso-1-cytochrome *c*

As mentioned in the Introduction, numerous positions of cc have been mutated to investigate their effects on the reduction potential. In this work we chose to calculate the effects of seven mutations, Arg38 → Lys, His, Asn, and Ala, Tyr48 → Phe, Asn52 → Ile, and Phe82 → Ser, using the continuum model. These mutations were chosen because they are known to preserve the structure of the wild-type protein. The X-ray structures of both reduced and oxidized cc's have been solved to high resolutions by Brayer and co-workers[36,37] (Brookhaven Protein Data Bank entries 1ycc and 2ycc, with resolutions of 1.2 and 1.9 Å, respectively). They also solved the X-ray structures of the Ile52 and Ser82 mutants in the reduced state (the former[8] to a resolution of 1.9 Å and the latter[4] to a low resolution of 2.8 Å). The overall average deviation between the backbone atoms of either mutant and those of the wild type is very small, ~0.26 Å. For the mutations at positions 38 and 48, Thurgood and collaborators[38,39] used NMR to investigate their structural consequences. They found that the mutation at either position did not significantly perturb the rest of the protein and that any conformational change was primarily localized at the site of mutation. The locations of the four mutated residues relative to the heme are shown in Figure 2. Residues Arg38 and Tyr48 are near the pyrrole-ring A propionate of the heme, residue Asn52 is between the pyrrole-ring A and D propionates, and residue Phe82 is near the CBB methyl of the heme.

Taken together, the seven mutations studied in this work involve a wide range of factors that determine the reduction potential: the charge and polarity of a surface residue (position 38), the polarity of an interior residue (position 48 or 52), and the size of a residue which controls the solvent exposure of the heme (position 82). The changes in reduction potential due to these mutations thus present a demanding set of data. A

(30) Zhou, H.-X. *Biophys. J.* **1993**, *65*, 955–963.
(31) Zhou, H.-X. *J. Chem. Phys.* **1994**, *100*, 3152–3162.
(32) Zhou, H.-X. Unpublished work.
(33) Jorgensen, W. L.; Tirado-Rives, J. *J. Am. Chem. Soc.* **1988**, *110*, 1657–1666.
(34) Northrup, S. H.; Pear, M. R.; Morgan, J. D.; McCammon, J. A. *J. Mol. Biol.* **1981**, *153*, 1087–1109.
(35) Churg, A. K.; Weiss, R. M.; Warshel, A.; Takano, T. *J. Phys. Chem.* **1983**, *87*, 1683–1694.
(36) Louie, G. V.; Brayer, G. D. *J. Mol. Biol.* **1990**, *214*, 527–555.
(37) Berghuis, A. M.; Brayer, G. D. *J. Mol. Biol.* **1992**, *223*, 959–976.
(38) Thurgood, A. G. P.; Pielak, G. J.; Cutler, R. L.; Davies, A. M.; Greenwood, C.; Mauk, A. G.; Smith, M.; Williamson, D. J.; Moore, G. R. *FEBS Lett.* **1991**, *284*, 173–177.
(39) Thurgood, A. G. P.; Davies, A. M.; Greenwood, C.; Mauk, A. G.; Smith, M.; Guillemette, J. G.; Moore, G. R. *Eur. J. Biochem.* **1991**, *202*, 339–347.

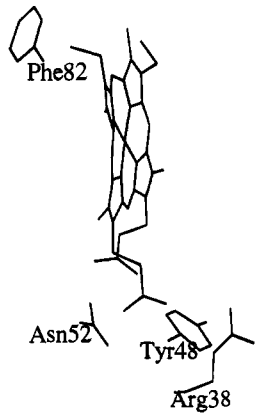

Figure 2. Locations of the four mutated residues relative to the heme in yeast iso-1-cytochrome *c*.

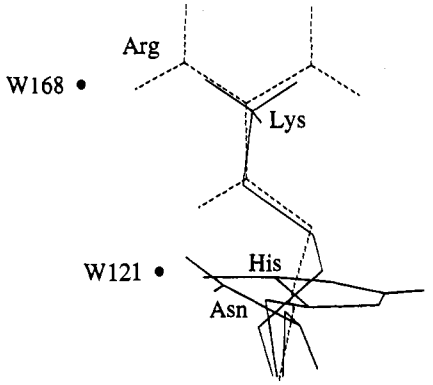

Figure 3. Side-chain conformations of the position-38 residues in the wild type (dashed lines) and the mutants (solid lines) of yeast iso-1-cytochrome *c*. All side chains are shown as they emerge from the CA atom in the backbone (bonds to polar hydrogens are included). NE and NH1 of Arg38 form hydrogen bonds with Wat121 and Wat168, respectively, while ND1 of His38 and ND2 of Asn38 both form hydrogen bonds with Wat121. The CA−CB bond of Ala 38 is almost superimposable on that of Arg38 and is not shown for clarity. The heme is to the left of the position-38 residues.

reasonably good reproduction of this set of data should demonstrate the capability of the continuum model.

A. Mutations at Position 38. In wild-type cc, the side chain of Arg38 interacts with the heme pyrrole-ring A propionate through the mediation of two water molecules,[36,37] Wat121 and Wat168 (see Figure 3). Because of this role of Wat121 and Wat168, they were included in the calculations. The geometry and charges of water molecules used were those of the TIP3P model.[40] The positions of the hydrogens on Wat121 and Wat168 were generated from the positions of heavy atoms and considerations of optimal hydrogen bonding.[36,37] Specifically, the first hydrogen of Wat121 (Wat168) was put on the line between the oxygen atom of the water molecule and the O1A atom of the pyrrole-ring A propionate, while the second hydrogen was located such that its distance to the backbone oxygen atom of His39 (Asn31) was minimized.

Cutler *et al.*[7] have measured the changes in reduction potential resulting from mutating Arg38 into Lys, His, Gln, Asn, Leu, and Ala in 0.1 M NaCl and 0.1 M sodium phosphate at pH = 7 and $T = 298$ K. Out of these six mutants, we chose the ones that have a lysine (a charged residue), an asparagine (a polar residue), and an alanine (a nonpolar residue) at position 38. The His38 mutant is also of interest because usually a histidine is unprotonated at pH = 7 but the His38 residue was found to be protonated[7] (possibly due to interactions with the pyrrole-ring A propionate). We thus included the His38 mutant to investigate the effect of protonation.

(40) Jorgensen, W. L.; Chandrasekhar, J.; Madura, J. D.; Impey, R. W.; Klein, M. L. *J. Chem. Phys.* **1983**, *79*, 926−935.

Table 1. Changes of Energy Contributions (kcal/mol) and Calculated and Experimental Reduction Potentials (mV) Due to Mutations in Yeast Iso-1-cytochrome *c*

mutation	$\Delta\Delta\mu^\circ_d$	$\Delta\Delta\mu^\circ_r$	$\Delta E^{\circ\prime}$(calcd)	$\Delta E^{\circ\prime}$(exptl)
		Arg38		
Lys	−0.18	0.01	−7	−23
His	−1.08	0.42	−28	−27
Asn	−6.56	5.47	−47	−34
Ala	−6.99	5.64	−58	−47
		Tyr48		
Phe	−0.39	0.01	−17	−22
		Asn52		
Ile	−1.18	−0.11	−56	−55
		Phe82		
Ser	−0.35	−0.38	−32	−35

No structure for any of the position-38 mutants are yet available, but NMR has provided the valuable information that a mutation at this position results in only a small conformational change close to the position itself.[38] Based on this information, we built the structure of each mutant by planting the particular mutation in the wild-type structure. Each mutant and the wild type thus had the same structure except for position 38. The conformation for the position-38 residue of each mutant was generated according to considerations of minimal structural perturbance and optimal hydrogen bonding (see Figure 3). The conformation of Lys38 was obtained by transplanting a lysine residue at another position that has the four backbone heavy atoms (N, CA, C, and O) and five side-chain heavy atoms (CB, CG, CD, CE, and NZ) best matched with the corresponding atoms (N, CA, C, and O from the backbone and CB, CG, CD, NE, and CZ from the side chain) of Arg38. The conformation of Ala38 was similarly obtained using the backbone atoms and the side-chain CB atom in the match. For Asn38 or His38, first a match was made by using the backbone atoms and the side-chain CB and CG atoms, then the rest of the residue was rotated around the CB−CG bond so an optimal hydrogen bond was formed between Asn38 ND2 or His38 ND1 and Wat121.

The Poisson and Poisson−Boltzmann equations for the wild type and the four mutants in the reduced and oxidized states were solved to find $\Delta\mu^\circ_{el}$, the electrostatic contribution to the change in standard chemical potential upon oxidation. As discussed in section II, the reduced and the oxidized states of each protein had the same structure while their charge distributions differed due to the unit charge gained upon oxidation, which was distributed among the heme atoms according to the calculation of Churg *et al.*[35] It should be further recalled that the total electrostatic contribution $\Delta\mu^\circ_{el}$ has a direct-action component $\Delta\mu^\circ_d$, due to the charge−charge interactions of the heme with the protein matrix, and a reaction-field component $\Delta\mu^\circ_r$, due to the dielectric boundary between the protein and the solvent. At an estimated ionic strength of $I = 0.335$ M (from 0.1 M NaCl and 0.1 M sodium phosphate), $\Delta\mu^\circ_d$ and $\Delta\mu^\circ_r$ for the wild type were found to be 31.91 and −29.60 kcal/mol, respectively, when the X-ray structure for the reduced protein was used. Notice that $\Delta\mu^\circ_r$ largely offsets $\Delta\mu^\circ_d$ to give a small total electrostatic contribution of $\Delta\mu^\circ_{el} = 2.31$ kcal/mol.

The changes in $\Delta\mu^\circ_d$ and $\Delta\mu^\circ_r$ due to the mutations of Arg38 → Lys, His (protonated), Asn, and Ala are listed in Table 1. From these energy changes one obtains the calculated changes in reduction potential due to the mutations, which are also listed along with the experimental results of Cutler *et al.*[7] in Table 1. The calculated and experimental $\Delta E^{\circ\prime}$ values show the same

ordering among the four mutants, Lys38 > His38 > Asn38 > Ala38, and the values for each mutation are also close. The variations of $\Delta E^{\circ\prime}$ among the mutants are dictated by the charge−charge interactions between the heme and the position-38 residues, which are strong for charged residues (Lys38 and His38), medium for a polar residue (Asn38), and weak for a nonpolar residue (Ala38). The dielectric boundary moderates the strengths of the charge−charge interactions but does not change the ordering of the strengths. The difference in $\Delta E^{\circ\prime}$ between Lys38 and His38 can be understood from their charge distributions (confer Figure 3). The charge of Lys38 is mainly located around the NZ atom. In protonated His38 the charge is shared between two centers, one around ND1, which has a distance roughly the same as that of the Lys38 NZ atom from the heme, and the other around NE2, which is farther away from the heme. This two-centered distribution weakens the charge−charge interactions with the heme and results in a decrease in reduction potential stronger than that from the Lys38 mutation. The difference in $\Delta E^{\circ\prime}$ between His38 and Asn38 is due to the protonation of His38. For an unprotonated His38, $\Delta E^{\circ\prime}$ was calculated to be −49 mV, virtually the same as the value −47 mV for Asn38. Finally the difference in $\Delta E^{\circ\prime}$ between Asn38 and Ala38 is due to the polarity of Asn38.

To check the sensitivity of the calculated results to the particular distribution used for the unit charge gained upon oxidation, we also investigated the consequences of putting the unit charge entirely at the heme iron. The resulting changes in reduction potential due to the four mutations were found to be $\Delta E^{\circ\prime}$ = −7, −28, −45, and −55 mV, respectively. Thus the results do not change at all for the Lys38 and His38 mutants and increase by only 2−3 mV for the Asn38 and Ala38 mutants. The small changes for the latter two mutants can be attributed to a slight weakening in the heme−Arg38 interactions in the wild-type protein upon adopting the new charge distribution.

Calculations were also made using the X-ray structure of the oxidized wild-type protein. The oxidized and reduced wild-type proteins have an average positional deviation of 1.1 Å between their corresponding atoms (including polar hydrogens and two water molecules, Wat121 and Wat168, a total of 1107 atoms). With the structure of the oxidized protein, $\Delta\mu^{\circ}_{d}$ and $\Delta\mu^{\circ}_{r}$ for the wild type were found to be 31.35 and −29.42 kcal/mol, respectively. The total electrostatic contribution of $\Delta\mu^{\circ}_{el}$ = 1.93 kcal/mol is slightly lower than the value 2.31 kcal/mol of the correspodning quantity found using the structure of the reduced protein. This is expected, as it should be easier to introduce a charge to the heme of the oxidized protein than to the heme of the reduced protein. The calculated changes in reduction potential due to the Arg38 → Lys, His, Asn, and Ala mutations are $\Delta E^{\circ\prime}$ = −6, −17, −49, and −65 mV, respectively. Compared to those obtained using the X-ray structure of the reduced wild-type protein (see Table 1), one sees that, despite the large structural differences, rather similar results are found. This adds confidence in the calculated results. Because of this similarity, for the rest of the section, only results calculated by using structures of the proteins in the reduced form will be presented. It is interesting to note that the reduction potentials of five species of cc (yeast iso-1, horse heart, tuna heart, turkey heart, and *Cabdida*) were found to be essentially identical at 262 ± 3 mV under the buffer conditions of T = 298 K, pH = 7, and I = 0.01 M.[41]

The reasonable performance of the continuum model in reproducing the experimental results on the effects of the position-38 mutations can be attributed to the inclusion of the reaction-field contribution due to the dielectric boundary between the protein and the solvent. This has been suggested by the qualitative analysis of section II on the effect of the charge and polarity of a surface residue. For example, upon the mutation of Arg38 → Ala, the 5.64 kcal/mol increase in $\Delta\mu^{\circ}_{r}$ largely offsets the 6.99 kcal/mol decrease in $\Delta\mu^{\circ}_{d}$ to give a small total decrease of 1.35 kcal/mol in $\Delta\mu^{\circ}_{el}$. This eventually makes the calculated decrease of 58 mV in reduction potential comparable to the experimental value of 47 mV. Cutler *et al.*[7] used the PDLD model to study the mutation of Arg38 → Leu, another nonpolar residue, and arrived at a similar attribution of the small decrease in reduction potential to the dielectric boundary between the protein and the solvent.

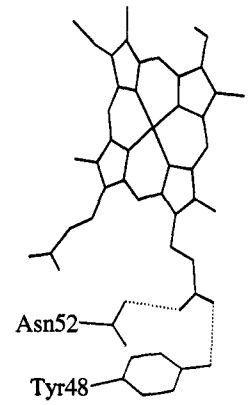

Figure 4. Hydrogen-bond interactions of the Tyr48 and Asn52 residues with the heme pyrrole-ring A propionate in yeast iso-1-cytochrome *c*. The structure is drawn using the X-ray coordinates of the reduced cc protein.

B. Mutation at Position 48. In wild-type cc, the hydroxyl group of Tyr48 forms a hydrogen bond with the O1A atom of the pyrrole-ring A propionate[36] (see Figure 4). The hydroxyl group results in a dipole moment of $p \approx 0.44$ *e*Å according to the OPLS parametrization,[33] which assigns partial charges of 0.435*e* and −0.700*e* to the hydrogen and oxygen atoms, respectively, and 0.265*e* to the antecedent carbon atom. In wild-type cc, the requirement to form a hydrogen bond with the O1A atom of the pyrrole-ring A propionate puts the hydroxyl dipole moment of Tyr48 in a direction that is only an angle of $\theta \approx$ 30° away from pointing at the heme iron. The hydroxyl group has a distance of $r \approx 9.0$ Å from the heme iron; thus, the direct interaction of the hydroxyl dipole with the heme charge gained upon oxidation contributes $(ep \cos\theta)/\epsilon_i r^2$ = 0.39 kcal/mol to $\Delta\mu^{\circ}_{el}$ of the wild-type protein. Deletion of the hydroxyl group through the Tyr48 → Phe mutation thus results in $\Delta\Delta\mu^{\circ}_{d}$ = −0.39 kcal/mol. These parameters were used in section II for the spherical-model analysis on the effect of the dipole of an interior residue. Within the spherical model, deleting an interior polar group that has no net charge does not result in any modification of $\Delta\mu^{\circ}_{r}$; thus $\Delta\Delta\mu^{\circ}_{d}$ constitutes the total change $\Delta\Delta\mu^{\circ}_{el}$. This would predict a 17-mV decrease in reduction potential.

Davies *et al.*[29] recently measured the change in reduction potential upon the Tyr48 → Phe mutation at T = 298 K and I = 0.006−0.008 M and found $\Delta E^{\circ\prime}$ = −22 mV. This is very close to the spherical-model result of $\Delta E^{\circ\prime}$ = −17 mV, caused by the loss of the heme−hydroxyl interaction. Calculations using the continuum model in which the detailed structures of the proteins were used gave essentially the same result. At I = 0.007 M, $\Delta\mu^{\circ}_{d}$ and $\Delta\mu^{\circ}_{r}$ for the wild type were found to be 31.22 and −28.97 kcal/mol, respectively. No structure for the Phe48 mutant is yet available, but NMR studies of Thurgood *et al.*[39] found that the mutation did not significantly perturb the rest of the protein. We thus generated the structure of the Phe48

(41) Margalit, R.; Schejter, A. *Eur. J. Biochem.* **1973**, *32*, 492−499.

mutant by transplanting a phenylalanine residue at another position that has the four backbone atoms (N, CA, C, and O) and seven side-chain atoms (CB, CG, CD1, CD2, CE1, CE2, and CZ) best matched with the corresponding atoms of Tyr48. The changes in $\Delta\mu^\circ_d$ and $\Delta\mu^\circ_r$ upon the mutation were found to be $\Delta\Delta\mu^\circ_d = -0.39$ and $\Delta\Delta\mu^\circ_r = 0.01$ kcal/mol (listed in Table 1). The near-zero value of $\Delta\Delta\mu^\circ_r$ is consistent with the spherical-model analysis.

Thurgood *et al.*[39] and Davies *et al.*[29] have proposed that the decrease in reduction potential upon the Tyr48 → Phe mutation was caused by increased electron density on the heme propionate after the loss of the hydrogen bond. The spherical-model analysis of section II and the detailed calculations described here suggest that no such elaborate scheme is required to explain the observed decrease in reduction potential. The decrease can come about simply due to the loss of the hydroxyl dipole of Tyr48.

We also investigated the effect of Wat121 and Wat168 by including them in the calculations. It was found that the only effect was to increase the values of $\Delta\mu^\circ_d$ for both the wild type and the mutant by 0.69 kcal/mol. With or without the two water molecules, the same value of −17 mV was found for $\Delta E^{\circ\prime}$.

C. Mutation at Position 52. The amide group of Asn52 in wild-type cc forms a hydrogen bond with the O2A atom of the pyrrole-ring A propionate[36] (see Figure 4). In the OPLS parametrization,[33] the C, O, N, atoms H atoms of the amide group $CONH_2$ have partial charges of $0.500e$, $-0.500e$, $-0.850e$, and $0.425e$, respectively. These result in a dipole moment of $p \approx 0.94$ eÅ. By forming a hydrogen bond with the O2A atom of the pyrrole-ring A propionate, the amide dipole of Asn52 is oriented at an angle of $\theta \approx 30°$ away from directly pointing at the heme iron. The amide group has a distance of $r \approx 8.0$ Å from the heme iron and thus contributes $(ep \cos \theta)/\epsilon_i r^2 = 1.06$ kcal/mol to $\Delta\mu^\circ_{el}$ of the wild-type protein.

When Asn52 is mutated to Ile, the amide dipole is lost. In the X-ray structure of the mutant,[8] the bulky Ile52 residue is found to also displace an internal water molecule, Wat166, which normally forms hydrogen bonds with Tyr67 and Thr78. This mutation was found to decrease the reduction potential of cc by 55 mV at pH = 7 and $I = 0.1$ M.[8,15]

Using their respective X-ray structures, we solved the Poisson and Poisson−Boltzmann equations to find $\Delta\mu^\circ_{el}$ values for the wild type and the mutant. For the wild type, Wat166 was included (the hydrogens were positioned such that optimal hydrogen bonds with OG1 of Thr78 and OH of Tyr67 were formed). At $T = 298$ K and $I = 0.1$ M, $\Delta\mu^\circ_d$ and $\Delta\mu^\circ_r$ for the wild type were found to be 31.50 and −29.48 kcal/mol, respectively. The changes in $\Delta\mu^\circ_d$ and $\Delta\mu^\circ_r$ upon the mutation were found to be $\Delta\Delta\mu^\circ_d = -1.18$ and $\Delta\Delta\mu^\circ_r = -0.11$ kcal/mol (listed in Table 1). These result in a change of $\Delta E^{\circ\prime} = -56$ mV in reduction potential, essentially reproducing the experimental result of −55 mV. The bulk of $\Delta E^{\circ\prime}$ comes from $\Delta\Delta\mu^\circ_d$, which in turn is primarily caused by the loss of the amide dipole of Asn52.

The X-ray structure of the Ile52 mutant presents an opportunity to check the appropriateness of using the generated structures in the calculations for the position-38 and -48 mutants. This is because we can use the same protocol to generate a structure for the Ile52 mutant and compare results obtained from the generated structure with those from the X-ray structure. Such a mutant structure was generated from the wild-type structure by transplanting an isoleucine residue at another position that has the four backbone atoms (N, CA, C, and O) and two side-chain atoms (CB and CG1) best matched with the corresponding atoms (N, CA, C, and O from the backbone and CB and OG1 from the side chain) of Asn52 (with Wat166 discarded). Using the generated structure, $\Delta\Delta\mu^\circ_d$ and $\Delta\Delta\mu^\circ_r$ were calculated to be −1.15 and 0.12 kcal/mol, respectively. These result in a change of $\Delta E^{\circ\prime} = -45$ mV in reduction potential. The major component $\Delta\Delta\mu^\circ_d$ is almost the same as found using the X-ray structure. The minor component $\Delta\Delta\mu^\circ_r$ has its sign reversed in comparison to the corresponding quantity found using the X-ray structure and accounts for a slightly worse agreement with experiment. The message from this comparison seems to be that, for a mutation which is known to cause conformational change only at the site of mutation, a generated structure such as one described above allows for a reproduction of the primary effect of the mutation in the calculation. A high-resolution structure of the mutant then provides further improvement of the calculated result.

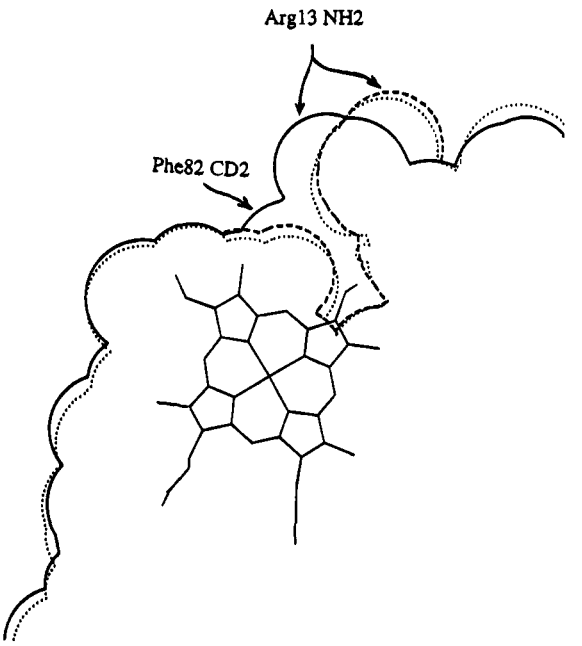

Figure 5. Superposition of the cross sections of yeast iso-1-cytochrome *c* and its Ser82 mutant through the phenyl ring of Phe82. The surface of the wild-type protein is drawn with solid arcs. The surface of the Ser82 mutant adopting the generated structure is drawn with dashed arcs; most of the surface is superimposable to the wild-type surface, the portion that is different exhibits the solvent channel in the mutant. The surface of the Ser82 mutant adopting the X-ray structure, after a match of the wild-type and mutant hemes, is drawn with dotted arcs. The heme is coplanar with the cross section but is actually 5 Å above. The exposed surfaces of the Phe82 CD2 and Arg13 NH2 atoms are indicated. The Arg13 NH2 atom moves away from the heme upon mutation.

Langen *et al.*[8] used the PDLD model to study the Asn52 → Ile mutation and arrived at a similar attribution of $\Delta E^{\circ\prime}$ to the loss of the amide dipole.

D. Mutation at Position 82. Phe82 is a residue which controls the exposure of the heme to the solvent. Mutation of Phe82 to a smaller Ser residue leads to the formation of a solvent channel which substantially increases the solvent exposure of the heme, as revealed by the 2.8-Å resolution X-ray structure of the mutant[4] (see Figure 5). Other major conformational changes are movement of the side chain of neighboring Arg13 and reorientations of the side chains of some distant residues, notably Trp59. The low resolution, due to the relatively small size of Ser82 mutant crystals obtainable, puts some uncertainty in the positions of the side chains. This uncertainty may overwhelm any small effect attributable to the mutation of Phe82 → Ser. To single out the effect of the mutation, we chose to generate a mutant structure by building into the wild-type

structure the side-chain conformations of those residues that undergo significant changes upon mutation. The residues selected were Arg13, Ser82, and Trp59. The conformation of each selected residue was generated by taking the conformation in the 2.8-Å resolution X-ray structure and planting it in the wild-type structure through a match of backbone atoms (N, CA, C, and O). The surfaces of the wild type and the Ser82 mutant adopting the generated and the X-ray structures are shown in Figure 5. It can be seen that the generated and X-ray structures of the mutant have very similar surfaces near the site of mutation.

Rafferty *et al.*[5] measured the change in reduction potential upon the Phe82 → Ser mutation at $T = 298$ K and $I = 0.1$ M and found $\Delta E^{\circ\prime} = -35$ mV. At these conditions, $\Delta\mu^{\circ}_{d}$ and $\Delta\mu^{\circ}_{r}$ for the wild type were found to be 31.22 and −29.43 kcal/mol, respectively. Using the generated mutant structure, the changes in $\Delta\mu^{\circ}_{d}$ and $\Delta\mu^{\circ}_{r}$ upon the mutation were found to be $\Delta\Delta\mu^{\circ}_{d} = -0.35$ and $\Delta\Delta\mu^{\circ}_{r} = -0.38$ kcal/mol (listed in Table 1). These give rise to a change of $\Delta E^{\circ\prime} = -32$ mV in reduction potential, very close to the experimental result of −35 mV.

The two components $\Delta\Delta\mu^{\circ}_{d}$ and $\Delta\Delta\mu^{\circ}_{r}$ have about equal shares in $\Delta E^{\circ\prime}$. The direct-action component $\Delta\Delta\mu^{\circ}_{d}$ arises from two contributions. The first is the interaction of the heme with the hydroxyl dipole of Ser82, which is directed away from the heme. The second is the movement of the Arg13 NE2 atom away from the heme upon mutation (see Figure 5), weakening the interaction of Arg13 with the heme. A further analysis of the reaction-field component $\Delta\Delta\mu^{\circ}_{r}$ revealed that it also arises from two contributions. The first is increased solvation of the heme upon mutation. This contribution has been emphasized by Louie *et al.*[4] and Rafferty *et al.*[5] The second is increased screening of the interactions of the heme with residues near the solvent channel. This contribution was discussed in section II. A particularly better screened interaction is the one with Arg13. As can be seen from Figure 5, solvent now gets in the path from the heme to the residue.

The conformational change of the Trp59 side chain was found to have minimal effect on the reduction potential. This conclusion was reached by calculations in which the conformation of Trp59 was kept at the wild-type one. $\Delta\Delta\mu^{\circ}_{r}$ was found to be the same as before, while $\Delta\Delta\mu^{\circ}_{d}$ had a rather small change of −0.05 kcal/mol.

As summarized in Table 1, the continuum-model calculations have reasonably reproduced the observed effects of seven mutations at four positions on the reduction potential of cc. These mutations involve a wide range of factors that determine the reduction potential. The reasonably good reproduction thus demonstrates the capability of the continuum model.

IV. Point Mutations in Yeast Cytochrome *c* Peroxidase

CCP is an enzyme that catalyzes the oxidation of ferro-cc by hydrogen peroxide. In this process, ferri-CCP first undergoes a 2-equiv oxidation by hydrogen peroxide into an intermediate called compound I [containing an oxyferryl (Fe^{4+}) heme and a Trp191 radical], which is then reduced in two subsequent 1-equiv steps by ferro-cc back to the native state.[42] In this work we deal with a much simpler process: the reduction of ferri-CCP to the ferrous state. Goodin and McRee[14] have recently measured the reduction potentials of the wild-type protein and three mutants that have Asp235 → Glu, Asn, and Ala replacements and found $E^{\circ\prime} = -183$, −113, −79, and −78 mV, respectively, at $T = 288$ K in 0.1 M potassium phosphate (pH = 7). They also solved the X-ray structures of the wild type and the Glu235 and Ala235 mutants in the ferrous state (Brookhaven Protein Data Bank entries 1cca, 1ccb, and 1ccc, with resolutions of 1.8, 2.1, and 2.0 Å, respectively). Previously Kraut and co-workers[43] have solved the X-ray structures of the wild type and the Asn235 mutant in the ferric state (Brookhaven Protein Data Bank entries 1ccp and 2ccp, respectively, both with a resolution of 2.2 Å). All three mutations, which occur at the interior position 235, are found to preserve the structure of the wild-type protein.

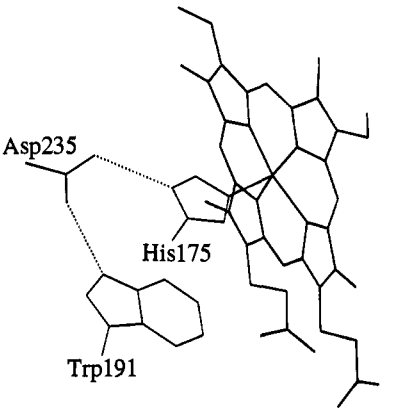

Figure 6. Hydrogen-bond interactions of the Asp235 carboxylate with the ND1 atom of His175 and the NE1 atom of Trp191 in yeast cytochrome *c* peroxidase.

The results on the reduction potentials of wild-type CCP and the three mutants create several puzzles. Both Asp235 and Glu235 have a carboxylate, yet the reduction potential of the mutant is 70 mV higher than that of the wild type. On going from Glu235 to Ala235, a buried carboxylate is lost; thus one may expect a large increase in reduction potential, yet the observed increase is only 35 mV. Similarly, on going from Asn235 to Ala235, an amide dipole is lost, yet the two mutants are found to have almost the same reduction potential. With the development of the dielectric continuum model in the previous two sections and the available X-ray structures for the wild type and the mutants, we can now attempt to solvent these puzzles.

Before calculations can be made, two issues have to be addressed. The first issue is the character of His175, which is liganded to the heme through the NE2 atom (see Figure 6). In wild-type CCP, the carboxylate of Asp235 forms a hydrogen bond with the ND1 atom of His175 (another hydrogen bond is formed with the NE1 atom of the Trp191 radical center, see Figure 6). Both resonance Raman spectroscopy[44] and NMR[45] have shown that the strong interaction with Asp235 serves to deprotonate His175 into an imidazolate. On the other hand, all three mutants have resonance Raman spectra that are characteristic of a normal imidazole in His175 (results quoted by Goodin and McRee[14]). On the basis of this information, for the wild type, we modeled the His175 side chain as an imidazolate and its hydrogen-bonding partner, the Asp235 side chain, as a carboxylic acid (see Figure 7). For each mutant, the His175 side chain was modeled as a normal imidazole (the Glu235 side chain was thus retained as a carboxylate, see Figure 7). Goodin and McRee[14] have suggested that the increase of 70 mV in reduction potential upon the Asp235 → Glu mutation might be accounted for by the change in His175 character from

(42) Kim, K. L.; Kang, D. S.; Vitello, L. B.; Erman, J. E. *Biochemistry* **1990**, *29*, 9150−9159.

(43) Wang, J.; Mauro, J. M.; Edwards, S. L.; Oatley, S. J.; Fishel, L. A.; Ashford, V. A.; Xuong, Ng.−h.; Kraut, J. *Biochemistry* **1990**, *29*, 7160−7173.

(44) Smulevich, G.; Mauro, J. M.; Fishel, L. A.; English, A. M.; Kraut, J.; Spiro, T. G. *Biochemistry* **1988**, *27*, 5477−5485.

(45) Satterlee, J. D.; Erman, J. E.; Mauro, J. M.; Kraut, J. *Biochemistry* **1990**, *29*, 8797−8804.

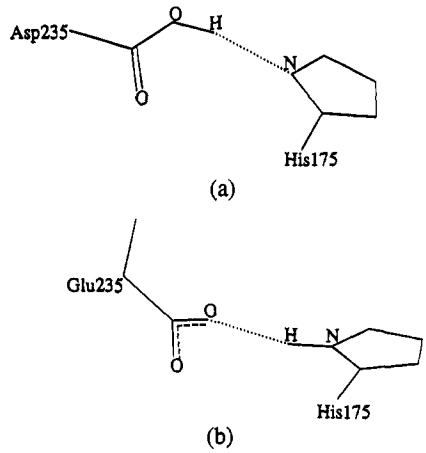

Figure 7. Protonation of His175 and the position-235 residue in (a) the wild type and (b) the Glu235 mutant of yeast cytochrome *c* peroxidase. The His 175 residue of either the Asn235 or the Ala235 mutant has the same protonation as that of the Glu235 mutant.

imidazolate to imidazole. Our calculations will test this suggestion quantitatively.

The second issue is the coordination of the heme iron. At neutral and low pH, the ferrous form of wild-type CCP and its mutants contains a five-coordinate iron.[44,46] The ferric form of wild-type CCP again contains a five-coordinate iron.[14,44] On the other hand, the ferric forms of the Ala235 and Asn235 mutants contain a six-coordinate iron, and the sixth ligand has been suggested to be a water molecule or a hydroxyl ion.[14,43-47] The ferric form of the Glu235 mutant also contains a six-coordinate iron, but the interaction of the iron with its sixth ligand is much weaker (derived from the observation[14] that the iron of the Glu235 mutant in the ferric form has high spin whereas the iron of either the Ala235 or the Asn235 mutant in the ferric form has low spin). The X-ray structures[43] of wild-type CCP and the Asn235 mutant in the ferric form provide information that is most useful for our calculations. It is found that the distance from the heme iron to the nearest water molecule, Wat595, decreases from 2.7 Å in the wild-type structure to 1.9−2.0 Å in the Asn235 mutant structure. We used the resulting change in the direct charge−dipole interaction between the heme and Wat595 to account for the effect of the sixth ligand. This contribution was included in the cases of the Asn235 and Ala235 mutants. It was not included in the case of the Glu235 mutant due to consideration of the much weaker interaction of the heme with its sixth ligand.

Using their respective X-ray structures, we solved the Poisson and Poisson−Boltzmann equations to find the electrostatic contribution $\Delta\mu^\circ_{el}$ to the oxidation-induced change in standard chemical potential for the wild type and the Glu235 and Ala235 mutants. At $T = 288$ K and $I = 0.235$ M (from 0.1 M potassium phosphate), the direct-action and reaction-field components of $\Delta\mu^\circ_{el}$ for the wild type were found to be $\Delta\mu^\circ_d = -72.06$ kcal/mol and $\Delta\mu^\circ_r = 57.27$ kcal/mol. The two components largely cancel to give a small net electrostatic contribution of $\Delta\mu^\circ_{el} = -14.79$ kcal/mol. Upon the mutation of Asp235 → Glu, the changes in $\Delta\mu^\circ_d$ and $\Delta\mu^\circ_r$ were found to be $\Delta\Delta\mu^\circ_d = 1.30$ kcal/mol and $\Delta\Delta\mu^\circ_r = 0.47$ kcal/mol. This results in a increase of 77 mV in reduction potential, close to the experimental value of 70 mV. Thus the change in His175 character from imidazolate to imidazole indeed accounts for the observed increase in reduction potential. The rest of the protein matrix was found to actually become more favorably interacting with the heme (due to movement of side chains of residues such as Trp51 and Lys90). Thus, if wild-type His175 was modeled as a normal imidazole, the Glu235 mutant would be found to have a lower reduction potential than the wild type, contradicting the experimental observation.

The changes in $\Delta\mu^\circ_d$ and $\Delta\mu^\circ_r$ upon the Asp235 → Ala mutation were found to be $\Delta\Delta\mu^\circ_d = 14.43$ kcal/mol and $\Delta\Delta\mu^\circ_r = -5.96$ kcal/mol. These results do not include the effect of the sixth ligand, i.e., they were obtained by using a five-coordinate heme for the mutant in both the ferrous and the ferric form. As mentioned earlier, we chose to account for the effect of the sixth ligand by the change in the direct charge−dipole interaction between the heme and Wat595. The energy arising from a charge−dipole interaction is given by $(ep \cos\theta)/\epsilon_i r^2$, where p is the dipole moment, θ is the angle between the dipole moment and the vector to the charge, and r is the distance to the charge. The dipole moment of a water molecule is about 0.5 eÅ. The distance r between Wat595 and the heme iron is 2.7 Å in the wild type and decreases to 1.9−2.0 Å in the mutant. The orientations of the Wat595 dipole in the wild type and the mutant are not known but should be directed away from the heme iron. For the purpose of calculation we assume that the dipole is directed at angles of 150° and 180°, respectively, from directing at the heme iron in the wild type and the mutant. The movement of Wat595 upon mutation is thus found to stabilize the ferric form of the mutant by ~6.0 kcal/mol. This amount should be subtracted from the earlier result for $\Delta\Delta\mu^\circ_d$, resulting in $\Delta\Delta\mu^\circ_d = 8.43$ kcal/mol. Combined with the earlier result of $\Delta\Delta\mu^\circ_r = -5.96$ kcal/mol, the reduction potential is predicted to increase 107 mV upon the Asp235 → Ala mutation, in agreement with the experimental result of 105 mV. While this agreement is not derived from a rigorous consideration of the sixth ligand (indeed its identity is still a subject of investigation), the calculations presented here serve to demonstrate its role in maintaining the reduction potential of the Ala235 mutant at a level that is only 105 mV above the reduction potential of the wild type, or only 35 mV above that of the Glu235 mutant. Without the effect of the sixth ligand, the reduction potential of the Ala235 mutant is predicted to be 290 mV higher than that of the Glu235 mutant.

The remaining question to be answered is why the reduction potentials of the Ala235 and Asn235 mutants are separated by only 1 mV. While we could have made detailed calculations on the Asn235 mutant to answer this question, we chose to directly look at the factor that has been shown to be the determinant for the change in reduction potential upon a mutation from a polar to a nonpolar residue at an interior position. This factor is the side-chain dipole of the polar residue, which in the present case is associated with the amide group of Asn235. The contribution of the amide dipole (magnitude $p = 0.94$ eÅ) to the change in $\Delta\mu^\circ_{el}$ on going from the polar to the nonpolar residue is $\Delta\Delta\mu^\circ_{el} = (-ep \cos\theta)/\epsilon_i r^2$, where θ is the angle between the dipole moment and the vector to the heme iron, and r is the distance to the heme iron. Only when θ is close to 90° can the value of $\Delta\Delta\mu^\circ_{el}$ be near zero. This is indeed what occurs in the Asn235 mutant. The angle between the amide dipole of Asn235 and the vector to the heme iron is ~100°. The distance between the amide dipole and the heme iron is ~7.5 Å, thus $\Delta\Delta\mu^\circ_{el} = 0.24$ kcal/mol. This would lead to an increase of only 10 mV in reduction potential, consistent with the small experimental value of 1 mV.

The results obtained through the continuum-model calculations concerning the mutations of Asp235 in CCP can be summarized as follows. The imidazolate character of the wild-

(46) Smulevich, G.; Miller, M. A.; Kraut, J.; Spiro, T. G. *Biochemistry* **1991**, *30*, 9546−9558.

(47) Vitello, L. B.; Erman, J. E.; Miller, M. A.; Mauro, J. M.; Kraut, J. *Biochemistry* **1992**, *31*, 11524−11535.

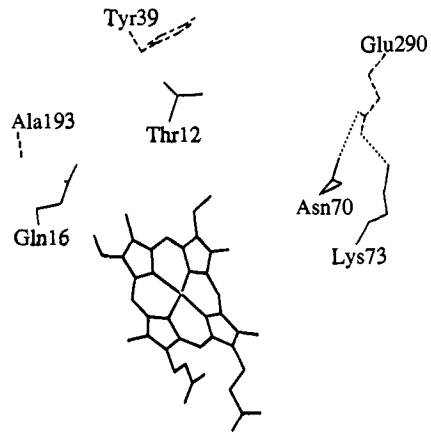

Figure 8. Residues in the interface between yeast iso-1-cytochrome *c* and cytochrome *c* peroxidase in the complex. The residues of cc are drawn with solid lines while those of CCP are drawn with dashed lines. Hydrogen bonds across the interface are drawn with dotted lines. The heme of cc is also shown.

type His175 is critical in lowering the reduction potential of the wild type 70 mV from that of the Glu235 mutant. A sixth ligand, such as a water molecule, is necessary for maintaining the reduction potential of the Ala235 mutant at a level that is only 35 mV above the reduction potential of the Glu235 mutant. That the Asn235 and Ala235 mutants have almost equal reduction potentials is due to the fact that the amide dipole of the Asn235 residue is oriented such that it does not stabilize or destabilize the charge on the heme.

V. Complex Formation and Electron Transfer

A. Complex Formation between cc and CCP. Rees[16] and Moore, Pettigrew, and Rogers[10] have suggested that, to facilitate electron transfer, the changes in protein environment upon complex formation (e.g., neutralization of oppositely charged residues) would change $\Delta\mu^\circ_{el}$ of both the donor and the acceptor so as to equalize their reduction potentials. The reduction potential of cc is ~270 mV, while the reduction potential of CCP is ~−190 mV. This would mean a combined change of 460 mV in reduction potential from cc and CCP upon complex formation. With the X-ray structure of the complex between cc and CCP now available,[17] we can use the continuum model to assess this suggestion.

Both cc and CCP are in the ferric state in the X-ray structure of the complex. In contrast to previous modeling, the interface of the cc:CCP complex is made mostly of van der Waals, instead of electrostatic, contacts (see Figure 8). Nevertheless a continuum-model study found that the electrostatic interactions between cc and CCP give rise to experimentally observed dependence of the binding constant of the proteins on ionic strength and mutations of charged residues.[32]

We solved the Poisson and Poisson−Boltzmann equations to find the electrostatic contribution $\Delta\mu^\circ_{el}$ to the oxidation-induced change in standard chemical potential for cc alone and in complex with CCP. At $T = 288$ K and $I = 0.235$ M, $\Delta\mu^\circ_{el}$ for cc alone was found to be 1.65 or 1.20 kcal/mol depending on whether the X-ray structure for ferro-cc[36] or ferric-cc[37] was used. Under the same conditions $\Delta\mu^\circ_{el}$ for cc in complex with ferric-CCP was found to be 0.48 kcal/mol. Complex formation with CCP thus results in a decrease of ~0.9 kcal/mol in $\Delta\mu^\circ_{el}$, corresponding to a decrease of only 40 mV in reduction potential. Comparison of the $\Delta\mu^\circ_d$ and $\Delta\mu^\circ_r$ components for cc in isolation and in complex with CCP reveals that the small difference in $\Delta\mu^\circ_{el}$ comes about because the difference in $\Delta\mu^\circ_d$ is largely offset by the difference in $\Delta\mu^\circ_r$.

As presented in the previous section, $\Delta\mu^\circ_{el}$ for CCP alone was found to be −14.79 kcal/mol. For CCP in complex with ferric-cc, $\Delta\mu^\circ_{el}$ was found to be −14.84 kcal/mol, virtually identical with the value of $\Delta\mu^\circ_{el}$ for CCP alone. Complex formation was thus found to have rather minor effects on the reduction potential of either cc or CCP. This is in direct contradiction with the suggestion of Rees[16] and Moore, Pettigrew, and Rogers.[10]

The finding that complex formation has rather minor effects on the reduction potentials of proteins has direct experimental support. In an early study of cc, Vanderkooi and Erecinska[18] found that complex formation with either CCP or cytochrome b_5 did not cause any measurable change in the reduction potential of cc. More recently Burrows *et al.*[15] studied the complex formation between cc and cytochrome b_5 and observed that upon complexation the reduction potential of either protein changed by less than 20 mV.

Further support is provided by the experimental observation[19,20] that the binding constants of ferro-cc (cc^{2+}) and ferri-cc (cc^{3+}) with ferri-CCP are very similar. The ratio, K_3/K_2, of the binding constants is related to the difference, $W_3 - W_2$, in the electrostatic interaction energies of ferro- and ferri-cc with CCP through[32]

$$-k_B T \ln(K_3/K_2) = W_3 - W_2 \tag{18}$$

The electrostatic interaction energy in turn is given by the difference, $G_{el}(cc^{s+}{:}CCP) - G_{el}(cc^{s+}) - G_{el}(CCP)$, $s = 2$ or 3, in electrostatic energy between the complex and the constituent proteins. Consequently

$$-k_B T \ln(K_3/K_2) = [G_{el}(cc^{3+}{:}CCP) - G_{el}(cc^{2+}{:}CCP)] - [G_{el}(cc^{3+}) - G_{el}(cc^{2+})] \tag{19}$$

The first term is just $\Delta\mu^\circ_{el}$ for cc in complex with CCP, while the second term is just $\Delta\mu^\circ_{el}$ for cc alone. Thus the fact that $K_3/K_2 \approx 1$ means that $\Delta\mu^\circ_{el}$ values for cc in complex with CCP and for cc alone are roughly the same.

B. Reorganization Energy of Biological Electron Transfer. The calculation of reduction potentials involves only equilibrium states, but the reorganization prior to the transfer of an electron necessarily involves nonequilibrium states; thus, it is not surprising that the condition for electron transfer cannot be simply expressed as the equalization of reduction potentials. A remarkable aspect of the electron-transfer theory of Marcus[21] is that the reorganization energy is related to quantities involving only equilibrium states. Marcus separated the reorganization energy λ into two parts, an inner part λ_i involving bond rearrangement of the redox centers and an outer part λ_o involving polarization reorientation of the surrounding environment. The Marcus theory has been very successful for dealing with electron transfer in small molecules,[22] where the outer reorganization occurs primarily in the solvent.

For electron transfer in proteins, the intervening protein matrices also have to reorganize. It is still not clear what is the proper way to account for the reorganization of protein matrices within a continuum model.[23] In addition, no simple methods have been found for obtaining the inner reorganization energy. Below we present our attempt. While it has become possible to find the reorganization energy of biological electron transfer using either classical molecular dynamics[48] or quantum[49]

(48) Schulten, K.; Tesch, M. *Chem. Phys.* **1991**, *158*, 421−446.
(49) Zheng, C.; McCammon, J. A.; Wolynes, P. *Chem. Phys.* **1991**, *158*, 261−270.

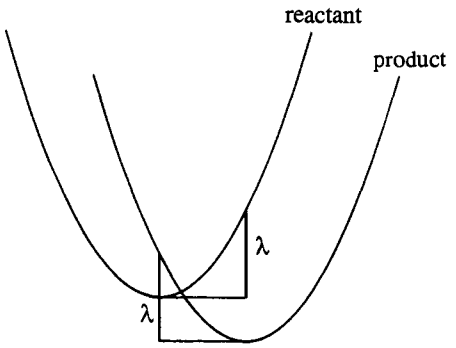

Figure 9. Energy surfaces of the reactant and product states in an electron-transfer reaction. The vertical lines indicate the reorganization energy.

simulations, these simulations are usually time consuming. A continuum-model-based method is thus still desirable.

The general expression of Marcus[21] for the outer reorganization energy is

$$\lambda_o = G_{el}(\epsilon_{op}) - G_{el} \tag{20}$$

where G_{el} is the electrostatic energy of the donor−acceptor complex embedded in the surrounding environment. The other term $G_{el}(\epsilon_{op})$ is the electrostatic energy of the donor−acceptor complex embedded in a medium with an optical dielectric constant (given by the square of the refractive index and due to the electronic polarization). In the complex, the electron donor bears a positive unit charge (which is gained upon oxidation) and the electron acceptor bears a negative unit charge. In modeling electron transfer between two small molecules, two dielectric media have generally been used, ϵ_i for the small molecules and ϵ for the solvent [of course in calculating $G_{el}(\epsilon_{op})$, ϵ should be replaced by ϵ_{op}]. What is a matter of debate is the choice for ϵ_i (see the discussion of Brunschwig, Ehrenson, and Sutin[50]).

Here we argue that ϵ_i should be identified with ϵ_{op}. This is derived from the result that, if such a choice is made, two different approaches lead to the same λ_o. The first is the direct evaluation of eq 20. For the sake of simplicity, let us suppose that the charge, e, in the donor is localized at $\mathbf{r}_1$ and the charge, $-e$, in the acceptor is localized at $\mathbf{r}_2$. Evaluation of eq 20 then leads to

$$\lambda_o = -e[V_1 - V_1(\epsilon_{op})]/2 + e[V_2 - V_2(\epsilon_{op})]/2 \tag{21a}$$

$$= -eV_1^r/2 + eV_2^r/2 \tag{21b}$$

The reaction field V_1^r at $\mathbf{r}_1$ is the sum of the reaction fields of the charge e at $\mathbf{r}_1$ and the charge $-e$ at $\mathbf{r}_2$. Let these be V_{11}^r and V_{12}^r and let the two reaction fields at $\mathbf{r}_2$ be V_{21}^r and V_{22}^r, then

$$\lambda_o = -e(V_{11}^r + V_{12}^r)/2 + e(V_{21}^r + V_{22}^r)/2 \tag{22}$$

This is the result of the first approach.

The second approach is based on the usual interpretation of the reorganization energy using two equicurvature parabolic energy surfaces for the reactant and product states (see Figure 9). In the reactant state, the electron charge, $-e$, is located at $\mathbf{r}_1$ while no charge is present at $\mathbf{r}_2$. In the product state, the electron charge is located at $\mathbf{r}_2$ while no charge is present at $\mathbf{r}_1$. The reorganization energy is given by the increase in energy along the reactant surface on going from the minimum of the reactant surface to the minimum of the product surface. Within the continuum model this quantity is given by the work done in the hypothetical process of moving the electron charge $-e$ from $\mathbf{r}_1$ to $\mathbf{r}_2$ against the original reaction field of the charge. This reaction field is $-V_{11}^r$ at $\mathbf{r}_1$ and $-V_{21}^r$ at $\mathbf{r}_2$, thus $\lambda_o = e(V_{21}^r - V_{11}^r)$. For two equicurvature parabolic surfaces, the same quantity is given by the increase in energy along the product surface on going from the minimum of the product surface to the minimum of the reactant surface. Within the continuum model this is given by $\lambda_o = e(V_{22}^r - V_{12}^r)$. To be consistent, we symmetrize the two continuum-model results and obtain

$$\lambda_o = e(V_{21}^r - V_{11}^r)/2 + e(V_{22}^r - V_{12}^r)/2 \tag{23}$$

This is the same as eq 22 after rearrangement.

The consistency of the results for λ_o from the two different approaches then suggests that the charges of the redox centers should be embedded in a medium with the optical dielectric constant ϵ_{op}. For electron transfer in small molecules, this medium is surrounded by the solvent with the dielectric constant ϵ. For electron transfer in proteins, the redox centers are surrounded by the protein matrices, with dielectric constant ϵ_i, which in turn are surrounded by the solvent. Thus we have a continuum model involving three dielectric media, as illustrated in Figure 10. In this model the outer reorganization energy λ_o is again given by any one of the equivalent eqs 20−23.

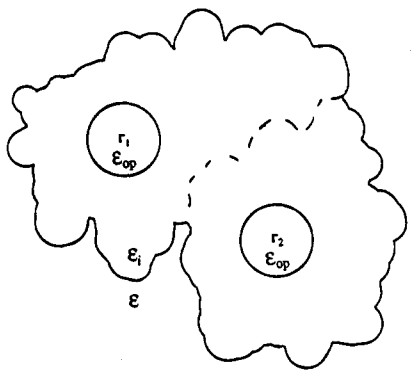

Figure 10. Continuum model for calculating the outer reorganization energy of electron transfer in a protein complex. The redox centers, represented by spheres, have dielectric constant ϵ_{op}. They are embedded in the protein matrices, which have dielectric constant ϵ_i (the dashed curve represents the interface between the donor and the acceptor). The protein complex in turn is embedded in the solvent, which has dielectric constant ϵ.

To rigorously calculate λ_o one has to solve the Poisson and Poisson−Boltzmann equations appropriate for the three dielectric media. Considering the uncertainty in the boundary between a redox center and a protein matrix, we have modeled the two redox centers as spheres (with an equal radius a and a separation $R = |\mathbf{r}_2 - \mathbf{r}_1|$; see Figure 10). Now let us calculate the reaction field of a charge e located at the center $\mathbf{r}_1$ of the first sphere. If the protein matrices are extended to infinity, then the electrostatic potential at any position $\mathbf{r}$ in the protein matrices is given by $e/\epsilon_i|\mathbf{r} - \mathbf{r}_1|$, provided $R \gg a$. This is $e/\epsilon_i a$ on the surface of the first redox center and $e/\epsilon_i R$ around the second redox center. After subtracting the direct-action component, the reaction field is found to be $(1/\epsilon_i - 1/\epsilon_{op})e/a$ at the first redox center and $(1/\epsilon_i - 1/\epsilon_{op})e/R$ at the second redox center. The outer reorganization in infinite protein matrices is then

$$\lambda_o^p = e^2(1/\epsilon_{op} - 1/\epsilon_i)(1/a - 1/R) \tag{24}$$

(50) Brunschwig, B. S.; Ehrenson, S.; Sutin, N. *J. Phys. Chem.* **1987**, *91*, 4714−4723.

This of course is a classical result of Marcus,[21] except the protein dielectric constant ϵ_i now takes the place of the solvent dielectric constant ϵ. The fact that ϵ_i is much closer to ϵ_{op} results in a much smaller reorganization energy. This advantage of biological electron transfer has been emphasized by Churg *et al.*[35]

When the outside of the protein matrices is replaced by the high dielectric solvent, additional reaction fields are induced at the redox centers. Provided the redox centers are not close to the dielectric boundary between the protein matrices and the solvent, these reaction fields are roughly the same as those obtained when the redox centers have the dielectric constant of the protein matrices. Consequently one gets back the previous continuum model involving only two dielectric media. We will call the additional reorganization energy λ_o^s.

Now we turn to the inner reorganization energy λ_i. As both λ_i and the $\Delta\mu^\circ_{cen}$ term of $\Delta\mu^\circ$, the oxidation-induced change in standard chemical potential, involve bond rearrangement of the redox centers, we suggest that λ_i is the sum of the $\Delta\mu^\circ_{cen}$ terms of the two redox centers:

$$\lambda_i = \Delta\mu_{cen}(1) + \Delta\mu_{cen}(2) \tag{25}$$

The $\Delta\mu^\circ_{cen}$ term in turn can be obtained from the measured reduction potential and the calculated $\Delta\mu^\circ_{el}$ term. This leads to

$$\lambda_i = ef[E^{\circ\prime}(1) + E^{\circ\prime}(2)] - [\Delta\mu_{el}(1) + \Delta\mu_{el}(2)] + C \tag{26}$$

where C is a quantity that is invariant from one electron-transfer reaction to another. The constant C is necessary because the reduction potentials are defined with respect to a particular standard electrode. Once a standard electrode is chosen (here, as in almost everywhere else, the choice is the normal hydrogen electrode) and the inner reorganization for one particular electron-transfer reaction is known, C can be determined.

The results of Cheung *et al.*[24] for the electron transfer from ferro-CCP to ferri-cc and from the anion radical of H_2 porphyrin cc to ferri-CCP can be used to obtain a reorganization energy of $\lambda = 37.0$ kcal/mol. We now use the analysis of the preceding paragraphs to find out the composition of this reorganization energy. The iron−iron separation in the cc:CCP complex is $R = 26.5$ Å. If a is taken to be 5 Å (the size of a heme) and ϵ_{op} is assigned a value of 1.8, the protein reorganization energy is found from eq 24 to be $\lambda_o^p = 16.5$ kcal/mol. By solving the Poisson and Poisson−Boltzmann equations, we found the solvent reorganization energy to be $\lambda_o^s = 3.5$ kcal/mol. The total outer reorganization energy is thus $\lambda_o = \lambda_o^p + \lambda_o^s = 20.0$ kcal/mol. If the redox centers are directly embedded in the solvent, the total outer reorganization energy is given by eq 24 but with the protein dielectric constant ϵ_i replaced by the solvent dielectric constant ϵ. The larger solvent dielectric constant would result in an outer reorganization energy of 29.2 kcal/mol. Other things being equal, the 9.2 kcal/mol increase in reorganization energy would lead to a 40-fold smaller rate for the electron transfer from ferro-CCP to ferri-cc. By virtue of the small dielectric constant, the protein matrices play an important role of reducing the reorganization energy from what would have been if the redox centers were embedded directly in the solvent and speeding up the electron transfer.

The difference between the 37.0 kcal/mol of total reorganization energy and the 20.0 kcal/mol of outer reorganization energy is the inner reorganization energy. The resulting value of $\lambda_i = 17$ kcal/mol for the electron transfer between cc and CCP allows the constant C in eq 26 to be determined. The reduction potentials of cc and CCP are about 270 and −190 mV, respectively, and the $\Delta\mu^\circ_{el}$ terms for the two proteins have been found earlier to be 1.4 ± 0.2 and −14.8 kcal/mol, respectively. Substituting these parameters into eq 26, one finds $C = 1.8$ kcal/mol.

To see whether this is a sensible approach, let us examine another electron-transfer reaction: the self-exchange in cc. The iron−iron spearation in a cc dimer is about 18 Å; eq 24 thus gives $\lambda_o^p = 14.7$ kcal/mol. The solvent reorganization energy should likewise be smaller than in the cc:CCP complex and thus should be between 0 and 3.5 kcal/mol. As such the exact value of λ_o^s is not very important. For concreteness let us assume that it scales as the iron−iron distance and obtain a value 2.4 kcal/mol. The total outer reorganization energy is thus $\lambda_o = 17.1$ kcal/mol. By substituting the reduction potential and $\Delta\mu^\circ_{el}$ term of cc and the value 1.8 kcal/mol just obtained for the constant C into eq 26, one finds $\lambda_i = 11.5$ kcal/mol. Thus the total reorganization energy is found to be $\lambda = 28.6$ kcal/mol. This is in surprising agreement with the experimental result of 28 kcal/mol found in two independent studies.[26] Churg *et al.*[35] have made calculations for the self-exchange in cc using a microscopic model. They found a solvent reorganization energy of 3 kcal/mol, in agreement with our estimate of 2.4 kcal/mol. However, they found much smaller values for the protein reorganization energy (2.4 kcal/mol) and the inner reorganization energy (1 kcal/mol). The resulting total reorganization energy of 6.4 kcal/mol is much smaller than the experimental result.

Using the present estimates, we can make some analysis on the difference in reorganization between the electron transfer from CCP to cc and the self-exchange in cc. Of the 9 kcal/mol difference in reorganization energy, about 6 kcal/mol is due to higher inner reorganization in the redox center of CCP and the remaining portion is due to higher outer reorganization around the redox centers in the cc:CCP complex. The higher inner reorganization for CCP may be justified considering the fact that the heme in CCP is anchored from only one side to the protein matrix (through the iron−His175 NE2 bond) whereas the heme in cc is anchored from both sides to the protein matrix (through iron−His18 NE2 and iron−Met80 SG bonds) (the heme vinyl groups in cc also form two thioether bonds with two Cys residues). The higher outer reorganization for the cc:CCP complex arises from the fact that the hemes in this complex are more isolated from each other (so the protein matrices and the solvent have to reorganize around two independent redox centers). A clearer picture on the relative importance of the various contributions (λ_i, λ_o^p, and λ_o^s) in a particular electron-transfer reaction may appear after additional results of reorganization energies are analyzed using the present approach. Experimental results are now available on the reorganization energies for the electron transfer from cytochrome b_5 to cc[25] and between the α and β subunits of hemoglobin[51] and for the self-exchange in myoglobin.[52]

VI. Conclusion

In this work we used the continuum model to study the effects of point mutations on the reduction potentials of cc and CCP. Qualitative analysis was presented to show that the model can account for a wide range of factors that determine the reduction potential. These include the charge and polarity of a surface residue, the polarity of an interior residue, and the size of a residue which controls the exposure of the heme to the solvent. The capability of the continuum model was demonstrated by a

(51) Peterson-Kennedy, S. E.; McGourty, J. L.; Kalweit, J. A.; Hoffman, B. M. *J. Am. Chem. Soc.* **1986**, *108*, 1739−1746.
(52) Crutchley, R. J.; Ellis, W. R.; Gray, H. B. *J. Am. Chem. Soc.* **1985**, *107*, 5002−5004.

reasonably good reproduction of a demanding set of data on cc, consisting of the measured differences in reduction potential between the wild type and seven mutants (Arg38 → Lys, His, Asn, and Ala, Tyr48 → Phe, Asn52 → Ile, and Phe82 → Ser).

Continuum-model calculations led us to the following results for CCP. The imidazolate character of the wild-type His175 is critical in lowering the reduction potential of the wild type 70 mV from that of the Glu235 mutant. A sixth ligand, such as a water molecule, is necessary for maintaining the reduction potential of the Ala235 mutant at a level that is only 35 mV above the reduction potential of the Glu235 mutant. That the Asn235 and Ala235 mutants have almost equal reduction potentials is due to the fact that the amide dipole of the Asn235 residue is oriented such that its does not stabilize or destabilize the charge on the heme.

The changes in reduction potential due to point mutations are small in general, yet it was possible to make reasonable calculations. A main reason is that we made sure that errors in involved quantities were properly canceled. A related issue is the quality of the X-ray structures used in the calculations. What is clear is that it is not meaningful to use a low-resolution X-ray structure in a calculation on the effect of a point mutation. A reasonable criterion for high resolution in the present context is one that is better than 2 Å. Unfortunately, the number of high-resolution X-ray structures is rather small, so it becomes necessary to generate structures. The generation of structures can be aided by such information as provided by NMR and resonance Raman spectroscopy. It is encouraging that such a generated structure for a mutant allows for a reproduction of the primary effect of the mutation, as evidenced by a comparison with the calculation using a high-resolution X-ray structure of the Ile52 mutant of cc.

Very similar results on reduction-potential changes $\Delta E^{\circ\prime}$, due to mutations of a charged residue into two other charged, a polar and a nonpolar residue, were obtained from two sets of structures that have an average positional deviation of 1.1 Å. This behavior is quite different from what have been observed in calculations of pK_a values of ionizable groups. For example, Oberoi and Allewell[53] found that pK_a values, obtained from two structures that were refined from the same set of X-ray data, differed by several pH units for several sites. An important difference between pK_a and $\Delta E^{\circ\prime}$ is that, while the former quantity is sensitive to all charge−charge interactions in the protein, the latter quantity is mainly determined by the interaction of the heme with the residue under mutation. In this context it is interesting to note that the reduction potentials of five species of cc were found to be essentially identical.[41]

The effects of complex formation were also studied in this work. Due to screening of the solvent, the presence of a second protein was found to have a rather minor effect on the reduction potential of the first protein. A consequence of this result is that not much error is introduced when the reduction potentials of the donor and acceptor in isolation are used to calculate the driving force for an electron-transfer reaction. The driving force technically is given by the reduction potentials of the proteins in complex.

Finally, the protein matrices were found to play an important role of reducing the outer reorganization energy from what would have been if the redox centers were embedded directly in the solvent and thus speeding up the electron transfer. By relating electron transfer to redox reactions, a method for obtaining the inner reorganization energy was proposed. A check against experimental results on the self-exchange in cc suggests that it is a promising attempt. Applications to other reactions will further test this method and help gain a better understanding on the nature of reorganization in biological electron transfer.

Acknowledgment. I thank Attila Szabo and A. Grant Mauk for helpful discussions and Gary D. Brayer for kindly sending me the X-ray coordinates of the Ile52 and Ser82 mutants of yeast iso-1-cytochrome *c*.

(53) Oberoi, H.; Allewell, N. M. *Biophys. J.* **1993**, *65*, 48−55.